Nanoscale

View Online
Dynamic Article Links

Cite this: *Nanoscale*, 2011, **3**, 1971

www.rsc.org/nanoscale

COMMUNICATION

Nanoscale porosity in pigments for chemical sensing

Jonathan W. Kemling and Kenneth S. Suslick*

Received 8th December 2010, Accepted 15th February 2011
DOI: 10.1039/c0nr00963f

Porous pigments in which chemically responsive dyes have been immobilized in a matrix of organically modified siloxanes (ormosils) have been prepared and characterized by AFM, TEM, EDS, and optical analysis. In typical chemical sensing applications, an array of 36 different porous ormosil pigments are deposited on polyethylene terephthalate (PET) film.

Sensing technology for toxic gases is important for both security and environmental monitoring.[1] Array-based sensing technology has emerged as a powerful approach toward the detection of chemically diverse analytes.[2] Based on cross-responsive sensor elements, array-based sensing systems mimic the mammalian gustatory and olfactory systems by producing specificity, not from any single sensor, but as a unique composite response for each analyte.[2–9] Previous electronic nose technologies, however, have required permanent sensor arrays, which therefore must employ weak chemical interactions (*e.g.*, physical adsorption or absorption) to avoid irreversible poisoning over time.

We have developed a rather different, but quite simple, optoelectronic approach[10–13] using a disposable colorimetric sensor array of chemically responsive dyes for the detection of a wide range of analytes, both in the gas phase[14,15] and in aqueous solutions.[16–18] The colors of many dyes are affected by a wide range of analyte–dye interactions (*e.g.*, pH, Lewis acid–base, dipolar, π–π, *etc.*); an array of such dyes can therefore be used to probe the chemical properties and reactivity of analytes and thereby discriminate among even closely similar analytes.

We have recently improved our array methodology by the use of chemically responsive nanoporous pigments created from the immobilization of dyes in ormosils and describe here their characterization. These pigments have been used in arrays for the detection of toxic industrial gases at ppb concentrations,[19–22] sugars and artificial sweeteners in aqueous solutions,[23,24] and even highly complex odorant mixtures (*e.g.*, coffee aromas).[25]

Our earlier sensor arrays used soluble molecular dyes in a semifluid polymer film that were printed onto a porous membrane. While effective, these semifluid arrays formulations suffered limited shelf-life from deterioration in response after storage; this was partly due to crystallization of the dyes and partly to chemical reactivity of the dyes while in solution. To tackle this deficiency, we have developed new nanoporous pigments for use in our sensing arrays. Here we discuss the properties of these materials which have substantially improved our colorimetric sensor array technology.

Porous sol–gel glasses provide excellent matrices for colorants due to their high surface area, relative inertness to both gases and liquids, good stability over a wide range of pH, and optical transparency.[26–28] In addition, the physical and chemical properties of the matrix (*e.g.*, hydrophobicity, porosity) can be easily modified by changing the sol–gel formulations. The use of these porous pigments significantly improves the stability and shelf-life of the colorimetric sensor arrays and permits direct printing onto non-permeable polymer surfaces. Additionally, we observe that the matrix serves as a pre-concentrator, improving the overall sensitivity.

The sol–gel matrices are prepared by acid-catalyzed hydrolysis of solutions containing commercially available silane precursors (*e.g.*, tetraethoxysilane (TEOS), methyltriethoxysilane (MTEOS), phenethyltrimethoxysilane, and octyltriethoxysilane (octyl-TEOS)) dissolved in low volatility solvents (*e.g.*, methoxyethanol, diethylene glycol dimethyl ether) that serve as porogens on the nanometre scale. After hydrolysis, chemically responsive indicators are added to the sol–gel solutions. For metalloporphyrin immobilization, the sol–gel solution uses a mixture of phenethyltrimethoxysilane and TEOS, and for acid or base indicators, TEOS with MTEOS or octyl-TEOS.

These final ormosil formulations with colorants are loaded into a multi-hole Teflon inkwell. A robotic printer (ArrayIt NanoPrint LM60) equipped with floating slotted pins (V&P Scientific, San Diego) delivers each solution by dipping into the inkwell and transferring ~130 nL of each formulation onto a PET film. The ormosil is allowed to cure under a slow stream of nitrogen for at least three days to allow full crosslinking and loss of the porogens, forming an ormosil xerogel. For most of our chemical sensing applications, a printed array of 36 different ormosil formulations is so generated, as shown in Fig. 1a.

After curing, the arrays are cartridged and used as sensor elements for the detection of a variety of analytes. Using a flatbed scanner, the array is imaged before and during exposure to an analyte. Each pigment responds differently to the change in the chemical environment, and by subtraction of the before exposure image from the after exposure image, a difference map can be generated (*i.e.*, red value minus red value, green minus green, blue minus blue, as shown in Fig. 2).[11–13] These difference maps provide a molecular fingerprint that is unique to any analyte or mixture of analytes at a specific concentration to which the array has been exposed.

Department of Chemistry, University of Illinois at Urbana-Champaign, 600 South Mathews Avenue, Urbana, Illinois, 61801, USA. E-mail: ksuslick@illinois.edu

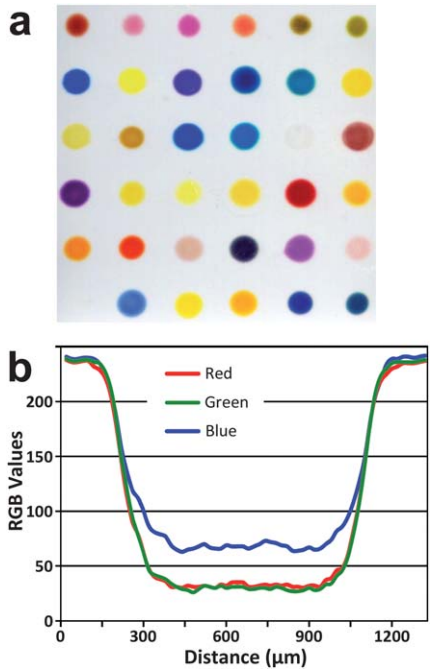

Fig. 1 (a) Image of a printed array, 2.5 × 2.5 cm. (b) RGB values of a linescan across the centre of a typical spot (#28, pyrocatechol violet; spots are numbered 1–6 along the top row, 7–12 in the second row, *etc.*).

Digital image analysis shows that the porous pigments have a uniform color distribution across the centre of the spot (Fig. 1). As an example of a typical spot, the centre 500 μm of the pyrocatechol violet spot (Fig. 1b, approximately 1 mm total diameter) have average RGB values of 31 ± 3, 28 ± 3, and 66 ± 3, respectively. For comparison, the white background in the immediate vicinity has RGB values of 235 ± 2, 238 ± 2, and 241 ± 2, respectively, which give a measure of the scanner reproducibility. These results quantitatively confirm excellent colorant dispersion across the porous pigment spot. The reproducibility of the optical densities of printed spots is excellent (typically in the same error limit range) and chemical sensing experiments use the difference between before-exposure and after-exposure images (Fig. 2), which further reduces errors in the pattern analysis.[15] Importantly, all image analysis for chemical sensing utilizes the average RGB values of the centre half of the spots to eliminate artifacts from the spot edges.

The pigment films were further characterized with a variety of analytical techniques. Scanning electron microscopy (SEM, JEOL JSM-7000F) and silicon Kα X-ray energy-dispersive spectroscopy (EDS) confirm that the silicon atoms in the ormosil matrix extend to

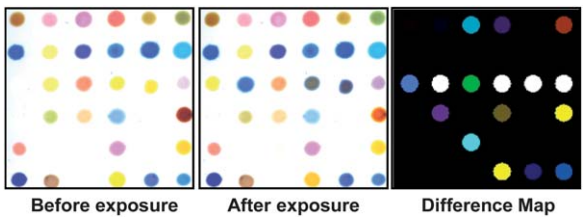

Fig. 2 Images of a 36-dye colorimetric sensor array before exposure, after two minutes of exposure to ammonia at its IDLH concentration at 298 K and 50% relatively humidity and the generated color difference map.[22]

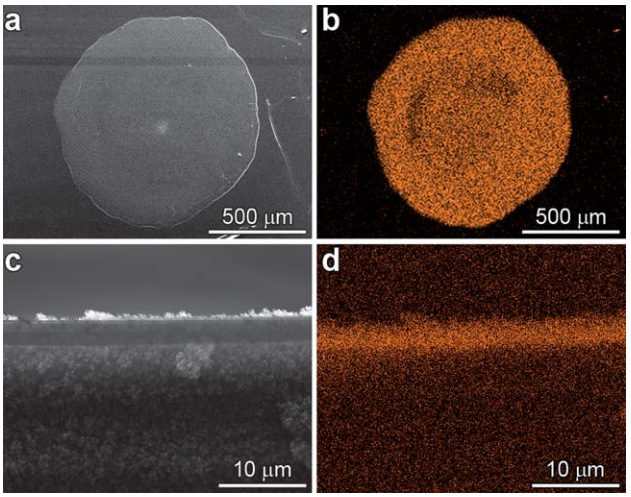

Fig. 3 SEM micrographs of a 1 mm diameter spot of porous pigment on PET film: (a) top surface and (b) EDS elemental mapping (Si Kα); (c) cross-section and (d) EDS elemental mapping (Si Kα). This pigment spot was made from a solution containing 6 mg of 5,10,15,20-pentafluorophenylporphyrinatozinc(II) in 1 mL of a hydrolyzed formulation of phenethyltrimethoxysilane and TEOS.

the outer edge of the colored spots (~1 mm diameter) and that the silicon concentrations are uniform throughout the spot area (Fig. 3a and b). EDS of a cross-section of the film shows that the thickness of the ormosil film is ~3 to 4 μm (Fig. 3c and d).

To confirm the film thickness, atomic force microscopy (AFM, Asylum Research MFP-3D) was performed on a spot that had one half removed by bisecting the spot and scraping it away with a sharp blade to reveal the PET substrate. The AFM topography map shows a step edge from the PET surface to the top of the spot of ~3.75 μm (Fig. 4). The ormosil thickness measured by AFM confirms the EDS film thickness estimate.

The AFM measurements also show ~50 to 200 nm spherical features on the surface of the film (Fig. 4 inset). Further analysis

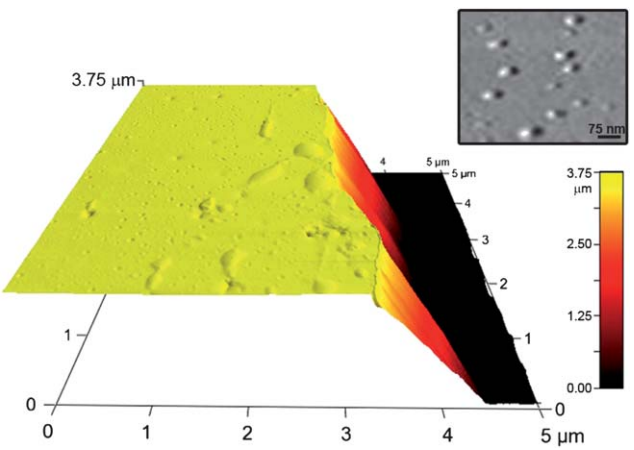

Fig. 4 AFM micrograph in perspective showing the height of the porous pigment at the spot centre compared to the base height of the PET as revealed by a scrape from a blade. Inset shows an enlargement of the surface pores (<100 nm). The pigment spot used here was made from 4 mg of bromocresol green in 1 mL of a hydrolyzed formulation of MTEOS and octyl-TEOS.

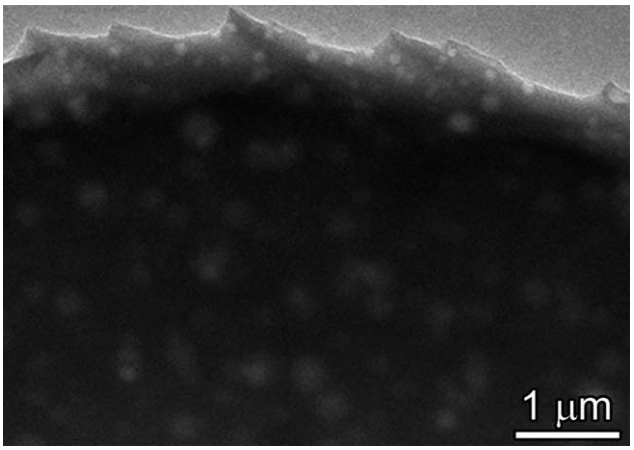

Fig. 5 TEM micrograph of porous pigment printed on PET film, which was then removed from the PET and placed on a TEM grid. The 50 to 200 nm features show the porosity created in these ormosil xerogels. The pigment had the same formulation as in Fig. 4.

under transmission electron microscopy (TEM, JEOL JEM 2100cryo) shows pores and void spaces in the material consistent with the size of the surface topographical features (Fig. 5). These pores and voids likely originate from micelle-like structures initially formed by the porogen (*i.e.*, low volatility solvent) and the hydrophobic groups on the trialkoxysilane precursors; after silanol condensation and solvent evaporation, voids and pores <100 nm are created in the rigid ormosil. The pores assist in mass-transport, and are responsible for the fast response times observed during sensing experiments (90% response generally occurs in <2 minutes).

Conclusions

We have prepared porous films of indicator doped ormosil organically modified siloxanes (*i.e.*, ormosils) for use in colorimetric sensor arrays. These pigments afford improvements in array shelf-life and stability without degrading analyte sensitivity[19–22] compared to films of plasticized polymers with dissolved dyes. After printing onto a non-porous polymer substrate (PET), the porous pigment films are ~1 mm in diameter and ~4 μm thick, with an even dispersion of colorant throughout the ormosil matrix. The fast response times observed in sensing of gas phase analytes are a result of ~50 to 200 nm pores in the porous ormosil xerogel, which we have been able to image using AFM and TEM.

Acknowledgements

This work was supported through the NIH Genes, Environment, and Health Initiative through award U01ES016011. Characterization was carried out in the Frederick Seitz Materials Research Laboratory Central Facilities, University of Illinois, which is partially supported by the U.S. Department of Energy under grant DEFG02-91-ER45439.

References

1 M. E. Byrnes, D. A. King and P. M. Tierno Jr, *Nuclear, Chemical, and Biological Terrorism—Emergency Response and Public Protection*, CRC Press, 2003.
2 J. W. Gardner and P. N. Bartlett, *Electronic Noses: Principles and Applications*, Oxford University Press, New York, 1999.
3 N. S. Lewis, *Acc. Chem. Res.*, 2004, **37**, 663–672.
4 F. Röck, N. Barsan and U. Weimar, *Chem. Rev.*, 2008, **108**, 705–725.
5 E. V. Anslyn, *J. Org. Chem.*, 2007, **72**, 687–699.
6 D. R. Walt, M. J. Aernecke, J. Guo and S. Sonkusale, *Anal. Chem.*, 2009, **81**, 5281–5290.
7 M. I. J. Stich, L. H. Fischer and O. S. Wolfbeis, *Chem. Soc. Rev.*, 2010, **39**, 3102–3114.
8 A. Berna, *Sensors*, 2010, **10**, 3882–3910.
9 C. Falconi, E. Martinelli, C. Di Natale, A. D'Amico, F. Maloberti, P. Malcovati, A. Baschirotto, V. Stornelli and G. Ferri, *Sens. Actuators, B*, 2007, **121**, 295–329.
10 N. A. Rakow and K. S. Suslick, *Nature*, 2000, **406**, 710–713.
11 K. S. Suslick, D. P. Bailey, C. K. Ingison, M. Janzen, M. E. Kosal, W. B. McNamaraIII, N. A. Rakow, A. Sen, J. J. Weaver, J. B. Wilson, C. Zhang and S. Nakagaki, *Quim. Nova*, 2007, **30**, 677–681.
12 K. S. Suslick, *MRS Bull.*, 2004, **29**, 720–725.
13 K. S. Suslick, N. A. Rakow and A. Sen, *Tetrahedron*, 2004, **60**, 11133–11138.
14 N. A. Rakow, A. Sen, M. C. Janzen, J. B. Ponder and K. S. Suslick, *Angew. Chem., Int. Ed.*, 2005, **44**, 4528–4532.
15 M. C. Janzen, J. B. Ponder, D. P. Bailey, C. K. Ingison and K. S. Suslick, *Anal. Chem.*, 2006, **78**, 3591–3600.
16 C. Zhang and K. S. Suslick, *J. Am. Chem. Soc.*, 2005, **127**, 11548–11549.
17 C. Zhang, D. P. Bailey and K. S. Suslick, *J. Agric. Food Chem.*, 2006, **54**, 4925–4931.
18 C. Zhang and K. S. Suslick, *J. Agric. Food Chem.*, 2007, **55**, 237–242.
19 S. H. Lim, L. Feng, J. W. Kemling, C. J. Musto and K. S. Suslick, *Nat. Chem.*, 2009, **1**, 562–567.
20 S. H. Lim, J. W. Kemling, L. Feng and K. S. Suslick, *Analyst*, 2009, **134**, 2453–2457.
21 L. Feng, C. J. Musto, J. W. Kemling, S. H. Lim and K. S. Suslick, *Chem. Commun.*, 2010, **46**, 2037–2039.
22 L. Feng, C. J. Musto, J. W. Kemling, S. H. Lim, W. Zhong and K. S. Suslick, *Anal. Chem.*, 2010, **82**, 9433–9440.
23 S. H. Lim, C. J. Musto, E. Park, W. Zhong and K. S. Suslick, *Org. Lett.*, 2008, **10**, 4405–4408.
24 C. J. Musto, S. H. Lim and K. S. Suslick, *Anal. Chem.*, 2009, **81**, 6526–6533.
25 B. A. Suslick, L. Feng and K. S. Suslick, *Anal. Chem.*, 2010, **82**, 2067–2073.
26 C. Rottman, G. Grader, Y. De Hazan, S. Melchior and D. Avnir, *J. Am. Chem. Soc.*, 1999, **121**, 8533–8543.
27 P. C. A. Jeronimo, A. N. Araujo and M. C. B. S. M. Montenegro, *Talanta*, 2007, **72**, 13–27.
28 H. Podbielska, A. Ulatowska-Jarza, G. Muller and H. J. Eichler, *Sol–Gels for Optical Sensors*, Springer, Erice, Italy, 2006.